Anisotropy of hole structures in polymers probed by two-dimensional angular correlation of annihilation radiation

Y. C. Jean, Y. Rhee, Y. Lou, H. L. Yen, H. Cao, K. Cheong, and Y. Gu
Department of Chemistry, University of Missouri–Kansas City, Kansas City, Missouri 64110
(Received 26 February 1996)

Two-dimensional angular correlation of annihilation radiation (2D-ACAR) experiments have been performed in a semicrystalline polymer, polyaryl-ether-ether-ketone. The two-dimensional hole structures of unstretched and stretched polymers, determined from the momentum distributions, are found to be spherical and ellipsoidal, respectively. The average hole radii are determined to be 2.6 Å in the unstretched sample and between 1.9 and 3.6 Å in the stretched sample. Applications of the 2D-ACAR method to image the three-dimensional hole, free-volume, and cavity structures of molecular systems are discussed.
[S0163-1829(96)12227-X]

I. INTRODUCTION

Application of polymeric materials to industry requires a basic understanding of materials properties. An important problem with polymeric materials is the existence of open free volumes and holes, which allow molecular relaxation. The size of these open spaces is on the order of sub-nanometer (i.e., Å). The determination of these atomic-scale free volumes and holes has been a challenge for materials scientists in recent years. Many experimental methods[1] have been applied to determine the physical properties of these atomic holes and only limited information about hole size, fraction, and shape is forthcoming.

In recent years, positron annihilation spectroscopy (PAS) is emerging as a useful technique to determine free-volume and hole properties of polymeric materials.[2] The unique property of the localization of the positronium atom, Ps (a bound atom between an electron and a positron), in an atomic hole ranging from a radius of 1 to 10 Å, makes PAS a sensitive probe for free-volume and hole characterization. A technique that provides a direct means of measuring hole size, fraction, and distribution is positron annihilation lifetime (PAL) spectroscopy. This is because there exists a one-to-one relationship between the observed *o*-Ps (the triplet state of Ps) lifetime and the hole dimension, and the formation probability of *o*-Ps is related to the number of holes in a polymeric material. However, this technique only provides the average hole dimensions but not the structure—particularly anisotropy.

Another PAS technique is the angular correlation of positron annihilation radiation (ACAR), which has been successfully used to probe the Fermi surface of metallic crystals.[3] ACAR monitors coincident 2γ radiation, which is a potential probe to determine hole structure in oriented polymeric materials when Ps is localized in the hole. We have reported a result for anisotropy of free-volume hole dimensions in a stretched polymer probed by one-dimensional ACAR (1D-ACAR).[4]

In this paper, we report a measurement of the two-dimensional structure of free-volume holes in semicrystalline polymer samples by using the 2D-ACAR method.

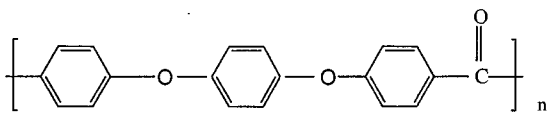

FIG. 1. Chemical structure of PEEK (polyaryl-ether-ether-ketone).

II. EXPERIMENTAL

A. Polymer samples

In a semicrystalline polymer, applying an external tensile is expected to result in a change in the hole shape from an isotropic to an anisotropic structure along the tensile orientation. A semicrystalline sample used in this study was prepared by isothermal treatment of an amorphous polyaryl-ether-ether-ketone (PEEK) supplied by Imperial Chemical, Inc., Americas (Wilmington, Delaware). Its chemical structure is shown in Fig. 1. The original 98+% amorphous PEEK has a glass transition temperature of 144 °C and density of 1.264×10^3 kg/m^3. The annealing was performed at 160 °C for 30 min. After annealing, the sample was slowly cooled down to room temperature. The crystallinity of the annealed sample was determined to be 23.0% by the density

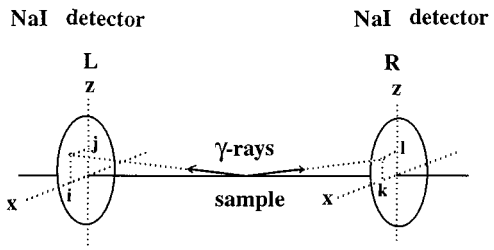

FIG. 2. A schematic diagram of 2D-ACAR spectrometer. The distance between the Anger camera (NaI detectors) and the sample (d) is 10 m. The momentum components p_x and p_z carried by 2γ rays detected in coincidence by the detector element L_{ij} and R_{kl} at coordinates (z_i, x_j) and (z_k, x_l) are given by $p_z=(z_i+z_k)$ mc/d; $p_x=(x_j+x_l)$ mc/d.

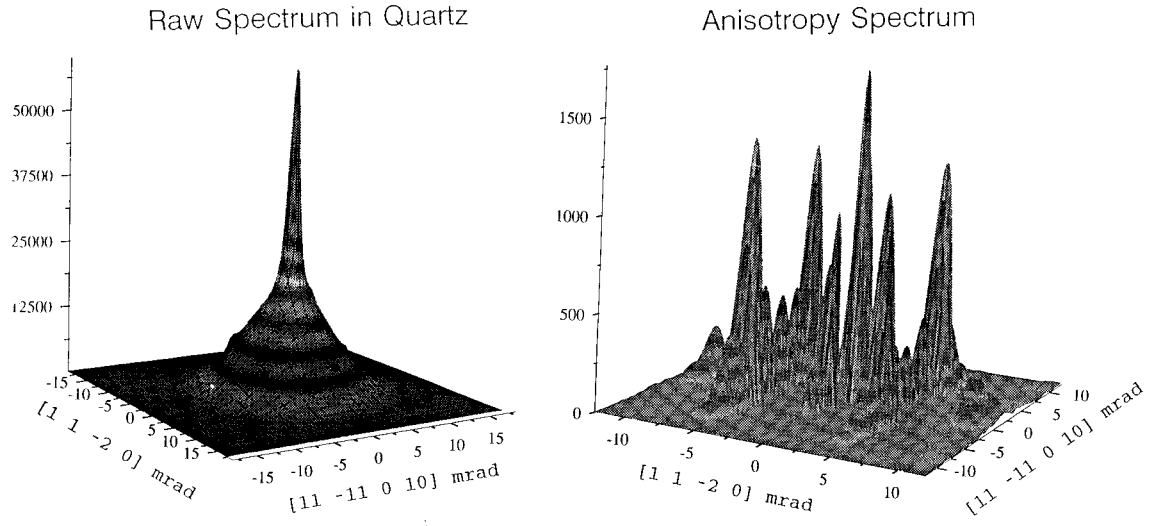

FIG. 3. 2D-ACAR raw spectrum and anisotropy plot in an oriented quartz crystal. The central peak of the raw spectrum is used to calculate the angular resolution. The satellite peaks in the anisotropy plot (right) correspond to p-Ps delocalization at the reciprocal lattice sites of the quartz crystal.

measurement (density$=1.293\times10^3$ kg/m^3). Detailed descriptions of sample preparation were given in another of our papers.[4]

One of the prepared PEEK samples was cut in a dog-bone shape and was then stretched uniaxially to a ratio of stretched to narrow axis of 2.60. Two 1-cm-wide and 1-mm-thick samples, one stretched and the other unstretched, were attached to the copper sample holder for the 2D-ACAR experiments.

B. 2D-ACAR spectrometer

Our 2D-ACAR spectrometer was the same one used at Brandeis University for measurement of momentum densities.[5] Figure 2 shows the geometry of the 2D-ACAR setup. The system consists of two Anger cameras (60-cm-diameter NaI detectors with 37 photomultipliers). The sample-detector distance is 10.0 m. The positron source is 50 mCi of ^{22}Na (DuPont model NER07), which is focused to the sample under a magnetic field of up to 2.0 T. The positron source is collimated by tungsten so that no prompt γ rays are detected by the camera. The coincident positron-electron photons by 2γ annihilation are registered and processed into 256×256 momentum matrices (p_x, p_z) according to the positions x and z from both cameras. The coincident counting rate is about 250 cps and the number of total counts of each spectrum is 1×10^8. 2D-ACAR spectra of each sample were recorded twice, once with and once without magnetic field, at room temperature. The data reported in this paper are those without the magnetic field. The effect of the magnetic field will be reported elsewhere.

The angular resolution of the 2D-ACAR spectrometer was determined by measuring the full width at half maximum (FWHM) of the central peak in the 2D-ACAR spectrum of an oriented quartz crystal.

C. Principle of two-dimensional momentum distribution

In a 2D-ACAR experiment, the experimental data represent a projection of the underlying three-dimensional electron-positron momentum density $\rho_{ep}(\mathbf{p})$:

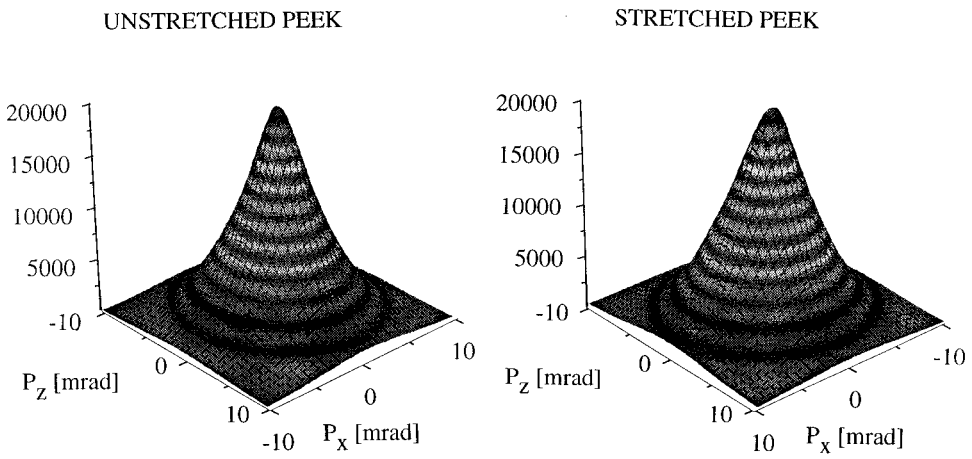

FIG. 4. 2D-ACAR raw spectra in unstretched and stretched PEEK semicrystalline samples. The difference seen between the two samples is due to the change of average hole structure from spherical in the unstretched sample to ellipsoidal in the stretched sample.

TABLE I. Angular resolution of 2D-ACAR. (1) The angular resolutions are determined from the FWHM's of the central peak of the sliced 1D spectra from a 2D-ACAR spectrum in an oriented quartz crystal (Fig. 1). (2) 0° corresponds to the sliced plane along the x axis. (3) 90° corresponds to the sliced plane along the z axis.

sliced angle (°)	FWHM (mrad)
0[2]	0.931±0.013
10	0.947±0.015
20	0.970±0.013
30	0.961±0.023
40	1.015±0.014
50	1.263±0.013
60	1.157±0.019
70	1.245±0.016
80	1.175±0.019
90[3]	1.181±0.019
100	1.252±0.019
110	1.268±0.016
120	1.172±0.028
130	1.158±0.018
140	0.944±0.018
150	1.023±0.015
160	1.052±0.014
170	0.987±0.016

$$N(p_x,p_z)=\text{const}\times\int \rho_{\text{ep}}(\mathbf{p})dp_y. \tag{1}$$

According to the Heisenberg uncertainty principle, the product of the momentum and space uncertainties is $\geqslant\hbar/2$. A 2D-ACAR spectrum contains the momentum distribution which arises from positron annihilation in a hole with a finite radius (R) in a polymer. Particularly, the p-Ps (the singlet state of Ps) self-annihilation contributes to the 2γ annihilation arising from the momentum uncertainty for a finite hole. This part of the annihilation contributes to near the central section of an ACAR spectrum. Therefore one expects to observe a correlation from an ACAR spectrum from a polymer sample: a larger hole results in a narrower momentum distribution while a smaller hole gives a broader momentum distribution. Since 2D-ACAR has a very good angular resolution, it is possible to accurately extract the information on hole size from an ACAR spectrum. The one-to-one relationship between the hole radius and the extent of the momentum uncertainty, $\theta_{1/2}$, near the center of an ACAR spectrum, can be expressed by the following equation:[6,7]

$$R=16.6/\theta_{1/2}-1.66, \tag{2}$$

where R and $\theta_{1/2}$ are expressed in the units of Å and mrad; respectively. The above equation is based on a simple model of the quantum particle p-Ps in an infinite potential well and an electron layer thickness.[6–9] The electron layer thickness was semiempirically determined by fitting the o-Ps lifetime with the known cavity size of the molecular system to be 1.66 Å as a part of Eq. (2) above.[10] The derivation of Eq. (2) can be found elsewhere.[7]

A 1D-ACAR spectrum can typically be fitted into three Gaussian functions. Each Gaussian gives a value of FWHM. The FWHM of the narrow component $\theta_{1/2}$, which is due to p-Ps annihilation, is used to determine R according to Eq. (2) (after deconvoluting via Eq. (3), described below). The 2D-ACAR spectrum obtained is sliced into a series of 1D-ACAR spectra at different crystallographic orientations. The 2D structure of holes in a polymer is then expressed as a series of sliced 1D-ACAR spectra with respect to the sample orientation. Each 1D-ACAR spectrum is fitted using the computer program ACARFIT.[11]

III. RESULTS AND DISCUSSION

A. Resolution functions

In 2D-ACAR, the angular resolution also depends on the location of detectors. It is important to determine the angular resolution of the 2D-ACAR spectrometer at different loca-

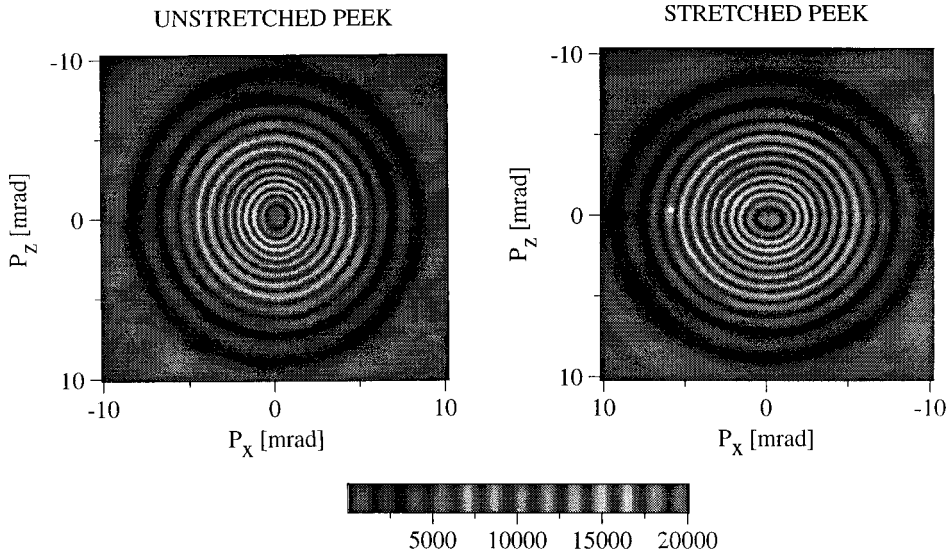

FIG. 5. Contour plots of 2D-ACAR raw spectra in unstretched and stretched PEEK samples. A narrowing of momentum density along z is due to the elongation of hole dimension.

TABLE II. 2D-ACAR results of unstretched PEEK.

Rotation (°)	$\theta_{1/2}$ (mrad)	R (Å)	I_1 (%)
0	3.912	2.58	8.848
	±0.051	±0.03	±0.032
10	3.918	2.58	8.167
	±0.051	±0.03	±0.031
20	3.922	2.57	8.282
	±0.051	±0.03	±0.031
30	3.920	2.57	8.879
	±0.051	±0.03	±0.031
40	3.935	2.57	8.814
	±0.051	±0.03	±0.031
50	4.004	2.49	8.371
	±0.051	±0.03	±0.031
60	3.971	2.52	8.610
	±0.051	±0.03	±0.031
70	3.999	2.49	8.000
	±0.051	±0.03	±0.031
80	3.978	2.51	8.885
	±0.051	±0.03	±0.031
90	3.979	2.51	8.796
	±0.051	±0.03	±0.032
100	4.000	2.49	8.411
	±0.051	±0.03	±0.031
110	3.994	2.50	8.797
	±0.051	±0.03	±0.031
120	3.976	2.52	8.933
	±0.051	±0.03	±0.031
130	3.972	2.52	8.554
	±0.051	±0.03	±0.031
140	3.915	2.58	8.356
	±0.051	±0.03	±0.031
150	3.934	2.56	8.221
	±0.051	±0.03	±0.031
160	3.944	2.55	8.517
	±0.051	±0.03	±0.031
170	3.944	2.55	8.884
	±0.051	±0.03	±0.031

TABLE III. 2D-ACAR results of stretched PEEK.

Rotation (°)	$\theta_{1/2}$ (mrad)	R (Å)	I_1 (%)
0	4.637	1.92	7.401
	±0.052	±0.03	±0.030
10	4.575	1.97	7.005
	±0.052	±0.03	±0.029
20	4.467	2.07	7.380
	±0.052	±0.03	±0.030
30	4.357	2.15	7.794
	±0.052	±0.03	±0.030
40	4.168	2.32	7.252
	±0.052	±0.03	±0.030
50	3.974	2.52	7.601
	±0.051	±0.03	±0.030
60	3.712	2.81	7.006
	±0.051	±0.03	±0.030
70	3.481	3.11	7.761
	±0.051	±0.03	±0.030
80	3.262	3.43	7.856
	±0.051	±0.03	±0.029
90	3.164	3.59	7.161
	±0.050	±0.03	±0.030
100	3.290	3.39	7.733
	±0.050	±0.03	±0.030
110	3.521	3.06	7.917
	±0.050	±0.03	±0.030
120	3.717	2.81	7.055
	±0.050	±0.03	±0.030
130	3.942	2.55	7.172
	±0.051	±0.03	±0.030
140	4.152	2.34	7.473
	±0.051	±0.03	±0.030
150	4.372	2.14	7.473
	±0.051	±0.03	±0.030
160	4.486	2.04	7.974
	±0.051	±0.03	±0.030
170	4.643	1.92	7.881
	±0.051	±0.03	±0.030

tions so that a more accurate hole dimension can be determined. We determine the angular resolution by measuring the 2D-ACAR spectrum in an oriented quartz sample. The 2D-ACAR spectrum and anisotropy plot of quartz are shown in Fig. 3. The satellite peaks represent the delocalization of p-Ps at the reciprocal lattice sites of quartz crystals. We resolve the sliced 1D-ACAR from the 2D-ACAR spectra into three Gaussians and obtain the FWHM values as a function of geometrical direction. The resulting angular resolution (in mrad) for 2D-ACAR spectrometers is listed in Table I. As shown in Table I, we obtain a better angular resolution along the x axis than the z axis because the positron annihilates at a shorter range on the x axis (which is the depth of the positron into the sample, ~0.1 mm than on the z axis (which is the positron beam size stopped on the sample, ~2 mm). The angular resolutions (Table I) are the actual experimental resolutions which contain geometry dispersions, detector resolutions, and positron thermal motion, and are used to extract the momentum broadening due to p-Ps localization in holes from the 2D-ACAR spectra in polymer samples.

B. 2D-ACAR spectra in PEEK polymers

We obtained 2D-ACAR spectra in two samples: one unstretched and one stretched PEEK. Figs. 4 and 5 show the raw 2D-ACAR spectra on three-dimensional and two-dimensional plots for both samples. The experiments were performed at room temperature and in ambient atmosphere. Each spectrum contains a total count of 1×10^8 over a period of 1 week of data acquisition. As shown in Figs. 4 and 5, we observe a spherical contour of 2D-ACAR spectra in the unstretched PEEK sample. However, in the stretched sample, we observe an ellipsoidal contour of 2D-ACAR spectra. In the unstretched sample, since the semicrystalline PEEK has

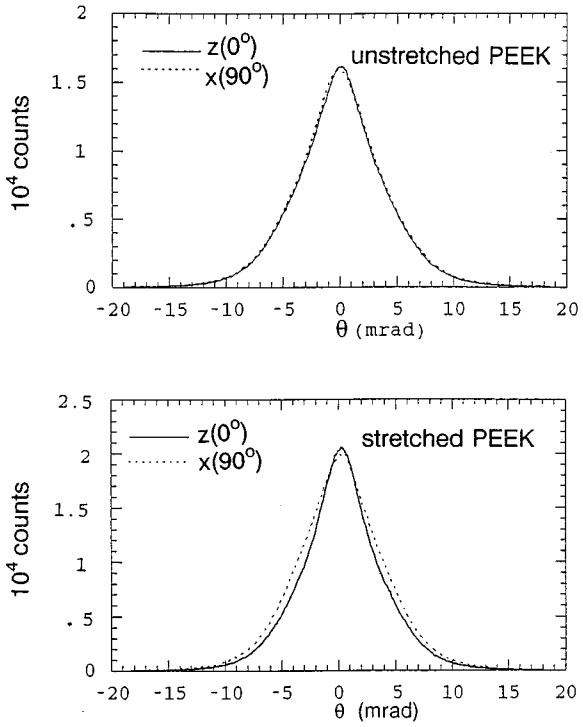

FIG. 6. 1D plot of 2D-ACAR spectra along x axis and (stretched) z axis. A narrowing of momentum density in the z direction is due to the stretching of holes along the z axis.

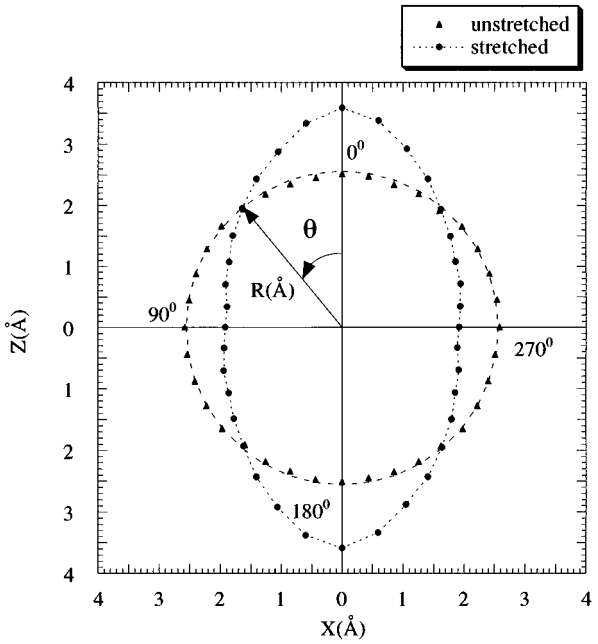

FIG. 7. Mean free-volume hole structures of unstretched and stretched PEEK samples. The stretched structure is ellipsoidal, while the unstretched one is spherical.

no crystallographic orientation, we expect the average hole structure to be isotropic. Therefore the 2D-ACAR spectrum is symmetrical with respect to p_x or p_z, although the individual hole may not be spherical. In the stretched sample, the hole is thought to align along the stretched direction (z), and thus the average hole structure is expected to be ellipsoidal, with a semimajor hole axis along the stretched direction (z) and a semiminor axis along the x direction. In an ellipsoidal hole model, the Ps wave function is distributed similarly to its hole structure.[11] According to the uncertainty principle, the long (semimajor) axis is expected to result in a smaller momentum uncertainty while the short (semiminor) axis is expected to have a larger one. As shown in Figs. 4 and 5, in a stretched sample, the positron-electron momentum density is seen to be ellipsoidal with a narrow distribution along the z direction. A clear difference in momentum distribution between the unstretched and stretched samples is obviously seen in the raw spectrum, particularly in Fig. 5. This observation is similar to the result of 1D-ACAR spectra obtained as a function of crystal orientation.[4]

The obtained 2D-ACAR spectra contain the two-dimensional hole structure perpendicular to the 2γ-ray direction. In order to obtain the two-dimensional hole structure, we process the 2D-ACAR raw data as follows: (1) The 2D-ACAR spectra are projected to 1D spectra along a rotation angle of momentum vector along p_x (p_x and p_z are denoted as 0° and 90° rotation, respectively, and x and z are the geometrical directions perpendicular to the annihilation γ-ray vector); (2) each 1D-ACAR spectrum is fitted into three Gaussians using the ACARFIT program in the PATFIT package;[11] (3) the FWHM of the narrow component of sliced 1D spectra, FWHM_1, is deconvoluted from the fit as a square sum:[12]

$$\mathrm{FWHM}_1^2 = (\theta_{1/2}) + \theta_r^2, \tag{3}$$

where θ_r is the angular resolution of 2D-ACAR spectrometer obtained in a quartz crystal (Table I); and (4) the radius of the hole along a specific orientation is calculated according to Eq. (2) and $\theta_{1/2}$. In the ACARFIT of the sliced 1D-ACAR spectra (each containing $\sim 10^6$ count), we find three Gaussian functions to give a reasonable χ^2 (<1.2). The FWHM's of the three Gaussians are 2–5, ~6.6, and ~16 mrad. Their corresponding intensities are found to be ~8%, 85%, and 7%, respectively. The narrow component of the ACAR spectrum is attributed to p-Ps annihilation of a free-volume hole while the intermediate and broad components are due, respectively, to positron (unbounded) annihilation and to some o-Ps pickoff annihilation. The results of the narrow component ($\theta_{1/2}$, after the resolution function is deconvoluted) for both unstretched and stretched samples are listed in Tables II and III. Our results of $\theta_{1/2}$ and I_1 are consistent with the previous 1D-ACAR data as a function of crystallographic orientation.[4] The sliced 1D-ACAR spectra along the x and z axes for both samples are plotted in Fig. 6. A clear narrowing of the ACAR spectrum along the stretched (z) axis is seen.

In Table II, we observe that $\theta_{1/2}$ is isotropic and the average hole radius $R = 2.54 \pm 0.03$ Å in the unstretched

TABLE IV. Comparison of PAL and ACAR results in PEEK.

	Unstretched	Stretched
R (ACAR)	2.54 ± 0.03 Å	1.92–3.59 ± 0.03 Å
$I_{p\text{-Ps}}$ (ACAR)	8.54 ± 0.05	7.45 ± 0.05
τ_3 (PAL)	1.785 ± 0.012 ns	1.632 ± 0.012 ns
$I_{o\text{-Ps}}$ (PAL)	18.1 ± 0.2	19.0 ± 0.20
R (PAL)	2.64 ± 0.10 Å	2.50 ± 0.10 Å

PEEK sample. In Table III, we observe that $\theta_{1/2}$ varies from 4.64 to 3.6 mrad and the average hole radius R varies from 1.92 to 3.59±0.03 Å in the stretched PEEK sample. The anisotropy of hole structure in the stretched PEEK is found to be 1.9±0.1. The obtained anisotropy of free-volume holes (=1.9) is less than the macroscopic stretched ratio of the z axis to the x axis (=2.6). This difference is understandable because 2D-ACAR measures the microscopic (atomic level) anisotropy, which in general is smaller than the macroscopic stretch ratio as the sample may relax after stretching. This smaller anisotropy in free-volume holes is consistent with the lifetime results as a function of eccentricity in a stretched PEEK sample.[13]

It is interesting to compare the 2D-ACAR results with the PAL results in the stretched PEEK samples. PAL gives the average hole size while 2D-ACAR gives additional anisotropy structure. Table IV shows a comparison between them. In the unstretched PEEK sample, hole radius results agree very well; in the stretched PEEK, the mean radius from PAL is consistent with the results from ACAR. The intensity of the narrow component from 2D-ACAR (I_1%) is slightly larger than one-third (the theoretical p-Ps to o-Ps ratio) of the $I_{o\text{-Ps}}$ obtained from PAL. This is probably due to the computer's fitting difficulty in separating p-Ps from positron components in 2D-ACAR spectra.

The complete two-dimensional hole structures obtained from 2D-ACAR are plotted in Fig. 7. The figure shows that the free-volume hole structure is spherical in the unstretched PEEK sample and ellipsoidal in the stretched PEEK sample.

CONCLUSION

We have demonstrated the use of 2D-ACAR in determining the anisotropy of free-volume hole structures in stretched PEEK semicrystalline polymers. The mechanically stretched PEEK (stretch ratio=2.6) has an anisotropy of hole structure of 1.9. It is thus possible to image the three-dimensional hole structure by performing 2D-ACAR experiments as a function of crystallographic orientation in molecular crystals.

ACKNOWLEDGMENTS

This research was supported by the NSF and the University of Missouri–Research Board.

[1] For example, see J. D. Ferry, *Viscoelastic Properties of Polymers*, 3rd ed. (Wiley, New York, 1980).

[2] For example, see Y. C. Jean, in *Positron Spectroscopy of Solids*, edited by A. Dupasquier and A. P. Mills, Jr. (IOS Press, Amsterdam, 1995), p. 563.

[3] For example, see R. N. West, in *Positron Spectroscopy of Solids* (Ref. 2), p. 75.

[4] Y. C. Jean, H. Nakanishi, L. Y. Hao, and T. C. Sandreczki, Phys. Rev. B **42**, 9705 (1990).

[5] S. Berko, in *Momentum Distributions*, edited by R. N. Silver and P. E. Sokol (Plenum, New York, 1989), p. 273.

[6] H. Nakanishi and Y. C. Jean, in *Positron and Positronium Chemistry*, edited by D. M. Schrader and Y. C. Jean (Elsevier, Amsterdam, 1988), Chap. 5.

[7] Y. C. Jean, Microchem. J. **42**, 72 (1990).

[8] S. J. Tao, J. Chem. Phys. **56**, 5499 (1972).

[9] M. Eldrup, D. Lightbody, and J. N. Sherwood, J. Chem. Phys. **63**, 51 (1981).

[10] H. Nakanishi, S. J. Wang, and Y. C. Jean, in *Positron Annihilation Studies of Fluids*, edited by S. C. Sharma (World Scientific, Singapore, 1988), p. 292.

[11] PATFIT package (1989), purchased from Risø National Laboratory, Denmark.

[12] It can easily be shown mathematically that two Gaussian functions with FWHM, $\theta_{1/2}$, and θ_r are convoluted to a single Gaussian function.

[13] Y. C. Jean and H. Shi, J. Non-Cryst. Solids **172-174**, 806 (1994).